Elasticity of hexagonal BeO

2001 J. Phys.: Condens. Matter 13 241

(http://iopscience.iop.org/0953-8984/13/2/302)

INSTITUTE OF PHYSICS PUBLISHING JOURNAL OF PHYSICS: CONDENSED MATTER

J. Phys.: Condens. Matter **13** (2001) 241–251 www.iop.org/Journals/cm PII: S0953-8984(01)16179-5

Elasticity of hexagonal BeO

V Milman[1] **and M C Warren**[2]

[1] Molecular Simulations Incorporated, The Quorum, Barnwell Road, Cambridge CB5 8RE, UK
[2] Department of Earth Sciences, University of Manchester, Oxford Road, Manchester M13 9PL, UK

Received 8 August 2000, in final form 7 November 2000

Abstract

We study the elastic properties, electronic structure, and equation of state of BeO using a first-principles pseudopotential method within the gradient-corrected approximation of the density functional theory. Comparison of the calculated and experimental properties of BeO shows good agreement for all the properties studied here: ground-state structure, linear and bulk compressibilities, and elastic moduli. Calculations are also performed with the local density approximation and the differences in elastic properties are interpreted in terms of a uniform compression. Analysis of the pressure effect on the lattice parameters and on the atomic coordinates shows that the structure changes are close to isotropic from zero to 100 GPa.

1. Introduction

Beryllium oxide is an exceptional member of the series of alkaline-earth oxides. It is the only one to crystallize in the wurtzite rather than in the rock-salt structure. Further, not only is BeO harder than the other alkaline-earth oxides but also it is among the hardest materials known. It is a good insulator like other alkaline-earth oxides, but its heat conductivity is an order of magnitude higher, which makes it a technically promising ceramic [1]. These interesting physical properties are related to characteristic features of interatomic bonding in BeO: for example, Compton scattering measurements revealed a significant covalent component of the primarily ionic bonding in BeO [2].

BeO (bromellite) crystallizes in the hexagonal wurtzite structure with the polar space group $P6_3mc$. There are two atoms of each kind in the unit cell on the special positions 2b: beryllium atoms at $(1/3, 2/3, 0)$ and oxygen at $(1/3, 2/3, z)$. The structure is thus defined by two lattice parameters, a and c, and the internal structural parameter, z. The determination of the z-parameter using x-ray diffraction is difficult for a number of reasons enumerated in reference [3]. However, as table 1 illustrates, there is a clear consensus regarding the ground-state structure of BeO. The atomic arrangement is very close to the 'ideal' wurtzite structure where the atoms of one hcp array occupy the exact centres of the tetrahedral voids of the other array. This would correspond to a c/a ratio of 1.633 and a z-parameter of 0.375, and so BeO is only slightly compressed along the z-axis relative to the ideal structure. The accepted values of a, c, and z are those reported in reference [10] (see table 1).

0953-8984/01/020241+11$30.00

Table 1. Theoretical and experimental data for structural parameters, the bulk modulus, and its pressure derivative for BeO; NCP: norm-conserving pseudopotential; USP: ultrasoft pseudopotential, AE: all-electron; HF: Hartree–Fock; PIB: potential-induced breathing model. The values of B and B' are evaluated from the fitting of the pressure–volume data to an analytical equation of state; the errors are obtained from the statistical analysis. Reference [10] provides the most accurate set of experimental data.

	a (Å)	c (Å)	c/a	z	B (GPa)	B'
USP-GGA[a]	2.701	4.387	1.624	0.3777	206(1)	3.33(4)
USP-LDA[a]	2.634	4.291	1.627	0.3776	220(1)	3.99(5)
NCP-GGA [4]	2.703	4.379	1.620	0.377	203	
NCP-LDA [4]	2.650	4.304	1.624	0.378	224	
NCP-LDA [5]	2.639	4.299	1.629	0.377	228	3.96
NCP-LDA [6]	2.664	4.324	1.623[b]		283	
AE-LDA [7]	2.665	4.352	1.633		230	
HF-LCAO [8]	2.697	4.361	1.617	0.3791	283	
PIB [9]	2.775	4.385	1.580	0.385	186	3.86
Experiment [10]	2.698	4.377	1.624	0.3781	210	5.1
Experiment [3]	2.698	4.277	1.585	0.3786		
Experiment [1]	2.699	4.385	1.625	0.3778		
Experiment [11]	2.6979	4.3772	1.6224	0.3778		
Experiment [12]	2.6979	4.3772	1.6224	0.3786		

[a] Present results.
[b] Fixed during calculation.

The first experimental measurement of the complete set of elastic coefficients of BeO was reported in reference [13], in which the pulse-echo method was used to determine the five independent elastic coefficients. The accuracy of the measurements was claimed to be better than 5%. However, a subsequent work [14] using essentially the same ultrasonic technique produced C_{12}- and C_{13}-stiffnesses that differed by 30–35% from the earlier results [13]; see table 2. It has been noted [14] that the $C_{66} \approx C_{44}$ relationship that follows from reference [13] is not reasonable for a hexagonal crystal. In a more recent study [15] an attempt has been made to derive low-temperature elastic coefficients from the temperature dependence of the x-ray Debye–Waller factor. The results obtained are close to those from reference [14], but the number of approximations in [15] makes it difficult to estimate the accuracy of the data obtained. BeO is the hardest of all II–VI compounds, and the existing controversy with regard to the accurate values of its elastic coefficients provides a major motivation for the present theoretical study.

There are two kinds of elastic coefficient: compliances, S_{ij}, describe the response of a material to an applied stress; conversely, stiffnesses, C_{ij}, give the stress required to maintain a given strain. Both stress and strain tensors have three tensile and three shear components. The linear elastic stiffnesses, C_{ij}, thus form a 6×6 symmetric matrix with a maximum of 21 different components, such that $\sigma_i = C_{ij}\varepsilon_j$ for small stresses, σ, and strains, ε. The number of independent non-zero elastic stiffnesses is usually lower due to the crystal symmetry. A hexagonal crystal has six different symmetry elements (C_{11}, C_{12}, C_{13}, C_{33}, C_{44}, and C_{66}), and only five of them are independent since $C_{66} = \frac{1}{2}(C_{11} - C_{12})$.

Computation of elastic coefficients provides a stringent test of the accuracy of the description of interatomic interactions. Empirical models are known to produce errors of the order of at least 10–15% for the diagonal components of the elastic stiffness tensor, and

Table 2. Elastic stiffnesses of BeO (GPa). The bulk modulus, B, is calculated from the elastic stiffness tensor. The errors are obtained from the statistical analysis of the results.

Method	C_{11}	C_{12}	C_{13}	C_{33}	C_{44}	C_{66}	B
USP-GGA[a]	439.1(3)	105(2)	72(1)	463(2)	142.1(5)	167(2)	204(1)
USP-LDA[b]	479(1)	113(1)	81(1)	510(2)	153.2(3)	183(1)	224(1)
USP-LDA[c]	396(2)	74(2)	51.5(5)	414(2)	139.4(5)	161(2)	173(1)
HF-LCAO [8]	526	110	92	556	148	208	244
PIB [9]	366	113	90	361	132	126	186
Ultrasonic [14]	460.6	126.5	88.5	491.6	147.7	167.0	224
Ultrasonic [13]	470	168	119	494	153	152	244
Debye–Waller [15][d]	468	130	120	497	148	169	240
Debye–Waller [15][e]	460	125	82	490	145	167	222

[a] Present results.
[b] Present results, based on the LDA-optimized structure.
[c] Present results, based on the experimental structure.
[d] Extrapolation to 0 K.
[e] Room temperature data.

the off-diagonal components are predicted even less reliably [16]. It is thus preferable to base the calculation of elastic coefficients on a quantum-mechanical description of the energetics of BeO.

The main driving force for the previous theoretical studies of BeO was to investigate pressure-induced phase transformation of the rock-salt structure. The present work is only concerned with the properties of the wurtzite modification of BeO, and so we will discuss previous theoretical results only for the ground state of the hexagonal phase.

One of the first computational studies of hexagonal BeO was undertaken using norm-conserving pseudopotentials and a plane-wave basis set [6]. At the time, this was a difficult system to study since solution of the density functional theory (DFT) equations required direct diagonalization of the Hamiltonian matrix and thus imposed much greater computational demands than modern methods. This explains why the authors had to restrict the number of k-points used to two. It was also necessary to use experimental values of the c/a ratio and of the z-parameter when constructing the theoretical equation of state. The calculated lattice parameters showed bond-length shortening typical for local density approximation, LDA, and the bulk modulus was significantly overestimated (table 1).

A semiempirical study of the structure and elastic coefficients of the wurtzite phase within the potential-induced breathing (PIB) model was presented in reference [9]. It is shown in tables 1 and 2 that this level of theory is not sufficient for an accurate description of the structure and properties of BeO, probably because of the covalent contribution to interatomic bonding.

A very accurate pseudopotential LDA study of six different structures of BeO has been performed in reference [5]. The calculations for the wurtzite phase were carried out with the energy cut-off of 1360 eV using 60 k-points in the irreducible part of the Brillouin zone. The results presented in table 1 show that this extreme accuracy does not improve agreement with experiment for ground-state structural properties compared to older less-accurate calculations [5]. However, the bulk modulus reported in reference [5] is significantly more reliable than the earlier theoretical estimates.

All-electron LDA calculations based on two different computational techniques were reported [7]. The results were obtained for a fixed c/a ratio and a fixed internal coordinate, z. This is a reminder of the fact that all-electron techniques often present enormous technical

difficulties when calculating forces and stresses. Thus, the pseudopotential approach becomes a method of choice for applications that require extensive use of the energy gradients, such as calculation of elastic coefficients.

In this paper, we report the results of a systematic DFT study of electronic, structural, and elastic properties of hexagonal BeO. The main goal is to resolve an existing controversy with respect to the values of the off-diagonal components of the elastic tensor.

2. Computational details

The quantum-mechanical calculations performed here are based on density functional theory [17, 18]. Exchange–correlation effects were taken into account using the generalized gradient approximation, GGA [19], as implemented in reference [20]. The GGA results for BeO properties have been shown to be more accurate than those calculated using the local density approximation [4]. We used the PBE form of the GGA [21], which was designed to be more robust and accurate than the original GGA formulation. Some of the calculations were repeated using the LDA exchange–correlation functional. The total-energy code CASTEP [22, 23] was used, which utilizes pseudopotentials to describe electron–ion interactions and represents electronic wavefunctions using a plane-wave basis set [24].

We used ultrasoft pseudopotentials [25], which require significantly less computational resources than norm-conserving potentials [26]. The pseudopotentials were generated using the PBE exchange–correlation functional. We elected to treat all four electrons of beryllium as valence since the cost of including 1s electrons is not large for modelling of the small unit cell of BeO.

The calculations were considered converged when the maximum force on atoms was below 0.01 eV Å^{-1} and the stress below 0.03 GPa. One set of calculations was carried out to produce the equation of state (EOS) of hexagonal BeO up to 100 GPa. In these runs, full geometry optimization was performed at a fixed value of applied hydrostatic pressure; this is similar to the experimental procedure for measuring the EOS. The calculated cell volumes were then used to construct the equation of state, which was fitted to a third-order Birch–Murnaghan equation to obtain the bulk modulus, B, and its pressure derivative, B'. While the entire pressure range of 0–100 GPa was used in the analysis of the structural changes, we only considered the results in the 0–30 GPa range when fitting the analytical equation of state. This affects the bulk modulus by no more than 4 GPa and its pressure derivative by no more than 0.2. The 30 GPa range was chosen as a representative of modern EOS studies using the diamond anvil cell technique [27]. The choice of the pressure values was such as to provide a denser set of points at small pressures to increase the fit quality of the analytical equation of state. This was achieved by using a non-uniform grid of pressure points. We used the step in pressures of 1 GPa up to 8 GPa, then a step of 2 GPa up to 14 GPa, 3 GPa up to 20 GPa, 5 GPa up to 50 GPa, and 10 GPa up to 100 GPa. Further calculations in the range of 100–200 GPa were carried out. These latter results are not discussed here since hexagonal BeO is not expected to be a stable phase at ultrahigh pressures [5].

The second set of calculations was performed to obtain elastic coefficients of BeO. Practical methods for determining the elastic coefficients from first principles usually set either the stress or the strain to a finite value, optimize any free parameters of the structure, and calculate the other property (strain or stress, respectively). With a careful choice of the applied deformation, elastic coefficients can then be determined. Applying a given homogeneous deformation (the strain) and calculating the resulting stress requires far less computational effort, since the unit cell is fixed and only the ionic positions require optimization. This is the method implemented in the present work. Two strain patterns, one with non-zero first

and fourth components, and another with a non-zero third component, give stresses related to all five independent elastic coefficients for the hexagonal system. Two positive and two negative amplitudes were used for each strain component with the maximum strain value of 0.6%, and then the elastic stiffnesses were determined from a linear fit of the calculated stress as a function of strain. This technique has been successfully utilized previously for a range of oxide materials including MgO [28], $MgSiO_3$ [29], and Li_2O [30].

3. Results and discussion

3.1. Convergence testing

Elastic coefficients, which describe the second derivatives of the total energy with respect to atomic displacements, are extremely sensitive to the details of the calculation. We therefore started by testing the convergence of our results with respect to calculation parameters, such as the size of the basis set and the quality of the Brillouin zone sampling.

The size of the basis set in the current approach is determined by the maximum kinetic energy for plane waves. An energy cut-off of 380 eV was used throughout this study. We tested convergence of the calculations by increasing the cut-off energy to 450 eV and found no difference in the calculated lattice parameters to within 0.001 Å. In fact, even an energy cut-off as low as 300 eV produces an adequate description of the structural parameters. We have used a reasonably large core radius for oxygen, 0.8 Å, when constructing the ultrasoft potential, which allowed us to obtain accurate results with such low values of the cut-off energy. We might note that the conventional norm-conserving pseudopotentials, even after optimization with respect to the required basis set size, require an energy cut-off as high as 1360 eV [5] or 1500 eV [4]. Even the extremely high cut-off energy of 2660 eV has been utilized during convergence testing [4]. It is clear that ultrasoft potentials provide the preferred route for studies of oxide systems more complex than an ideal BeO structure.

The Brillouin zone sampling was carried out using 48 k-points in the irreducible part, which corresponded to the $11 \times 11 \times 6$ set of Monkhorst–Pack points [31]. Further increase of the k-point density to 96 points of the $14 \times 14 \times 8$ Monkhorst–Pack set had no effect on calculated properties. Elastic stiffnesses, which are most sensitive to details of the calculation, changed by no more than 0.1% when comparing the results obtained with a 380 eV energy cut-off and 48 k-points to those obtained at 450 eV and 96 k-points.

3.2. Ground-state structure and electronic properties

The ground-state structure of hexagonal BeO as determined from the $P = 0$ GPa geometry optimization is given in table 1. We obtained both lattice parameters a and c within 0.003 Å of the experimental values [10], which illustrates the level of accuracy that can be achieved in the modern DFT calculations. The error in the internal coordinate, z, is also very small, 0.1%. These results represent the best description of the structure of BeO out of all currently available theoretical studies, including the all-electron calculations [7].

Comparison of LDA and GGA results shows that the LDA overbinding can be interpreted as a hydrostatic pressure applied to the system (approximately 14 GPa in this case). The same conclusion has been reached previously for such systems as elemental Se [32], As, and Sb [33]. The structure of BeO predicted using the LDA has 2% smaller lattice constants while there is very little distortion of the structure compared to the GGA prediction: the LDA and GGA values of c/a and z are very close. Both LDA and GGA data are quantitatively similar to the results obtained using norm-conserving pseudopotentials [4]. For example, the bulk modulus

calculated using the LDA is about 20 GPa higher than the GGA result (table 1). This can be attributed entirely to the difference between the equilibrium cell volumes obtained using these two approximations for the exchange–correlation potential, or, in other words, to the pressure dependence of the bulk modulus. If we treat the value of 220 GPa obtained using the LDA as a bulk modulus at $P = 14$ GPa, then the fitted equation of state will produce $B = 163$ GPa for the zero-pressure state. The pressure derivative of the LDA bulk modulus is calculated to be 4.0 (table 1), which corresponds to the 56 GPa change in bulk modulus over the 14 GPa pressure range. The difference between the two values quoted above (220 and 163 GPa) is 57 GPa, and it is thus accurately reproduced in the assumption of the linear dependence of the bulk modulus on pressure. The extrapolated value of the LDA bulk modulus, 163 GPa, agrees well with the results of the elastic coefficient calculations discussed below.

It is interesting that the present *ab initio* results for the BeO EOS agree well with the simplest ionic model based on the repulsive Born–Mayer potential between the atoms [34]. This model with parameters obtained from the empirical relationships between the properties and molecular volume of highly ionic materials predicts $B = 212$ GPa and $B' = 3.4(3)$ [34]. The pressure derivative of the bulk modulus is thus very close to the calculated GGA value of 3.33. On the other hand, the experimental data based on hydrostatic compression of single crystals [10] and on ultrasonic measurements on polycrystals [35, 36] give 5.1 and 5.5, respectively. A brief analysis suggests that the experimental EOS derived in reference [10] cannot be used to extract a reliable value of B'. These experimental data are equally well described using two sets of parameters of the third-order Murnaghan–Birch equation of state. If the fixed value of $B = 210$ GPa is used, then $B' = 5.1 \pm 1.0$ is obtained, while EOS fitting with the fixed value of $B' = 4$ produces $B = 212 \pm 3$ GPa [10]. This extreme insensitivity of the quality of the fit to the value of B' shows that better quality measurements over a wider pressure range are necessary if one is to make quantitative experimental conclusions regarding the pressure derivative of the bulk modulus.

The electronic band structure and density of states for BeO are presented in figure 1. Electronic properties of BeO have been studied extensively using the orthogonalized linear-combination-of-atomic-orbitals (OLCAO) method in the LDA framework [37]. Our results agree qualitatively with the description of the electronic structure given in [37]. The valence band of this wide-gap insulator consists of an s-character band at low energies, and a p-character band at higher energies. A direct gap at Γ was reported from the OLCAO calculations as 7.54 eV [37] compared to experimental values between 7 and 10.7 eV, in quite good agreement considering the usual band-gap underestimation within the DFT framework. We obtained an even higher value of 8.4 eV for this wide-gap insulator. It is likely that the improved description of the band-gap is due to the use of the GGA approximation as opposed to the LDA one.

3.3. Structural changes under pressure

The BeO structure scales isotropically under hydrostatic compression as was noted in the experimental study [10]. The linear compressibilities calculated from linear fits to the $a(P)$ and $c(P)$ dependencies from 0 to 3 GPa are practically identical for the two axes: $\beta_a = 1.51$ TPa^{-1}, $\beta_c = 1.48$ TPa^{-1}. These results are in excellent agreement with the experimental low-pressure data of 1.50(4) and 1.46(3) TPa^{-1}, respectively [10]. Note that the Hartree–Fock study gives 1.34 and 1.37 TPa^{-1} [8], while the PIB model gives 1.73 and 1.91 TPa^{-1} for linear compressibilities [9]. We further evaluated the linear compressibilities from higher-order polynomial fitting of the $a(P)$ and $c(P)$ data. We used a function of the form

$$a(P)/a_0 = 1 + \beta_a P + \sum_{n=2} k_n P^n.$$

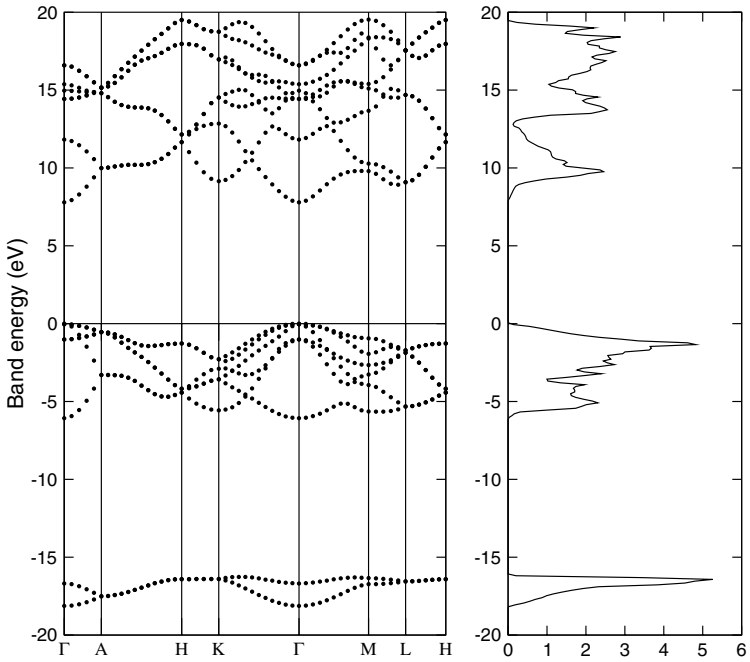

Figure 1. The band structure (left panel) and density of states (right panel) of hexagonal BeO.

This procedure was applied to the data over the same range of pressures as that used in the EOS fitting, and the results of $\beta_a = 1.63$ TPa^{-1}, $\beta_c = 1.62$ TPa^{-1} are statistically more reliable than the low-pressure linear fitting ones.

It follows from the above results that the c/a ratio is practically independent of pressure. Our data show that this ratio increases from 1.624 to only 1.627 over the 100 GPa pressure range. Analysis of the low-pressure data (figure 2) gives $\mathrm{d}(c/a)/\mathrm{d}P = 0.05$ TPa^{-1}, compatible with the experimental conclusion that the c/a ratio does not change with pressure [10]. Semiempirical results obtained using the PIB model give quite a different value for the pressure derivative of the c/a ratio, -0.29 TPa^{-1} [9]. This shows that the delicate pressure-induced structural changes in the BeO crystal can be only reproduced using full *ab initio* treatment.

The internal parameter z, the only other structural parameter that might be responsible for qualitative structural changes, is also unchanged under pressure. Experimental results give $\mathrm{d}z/\mathrm{d}P = 0.3 \pm 0.3$ TPa^{-1} [10], and our calculations show that the absolute value of $\mathrm{d}z/\mathrm{d}P$ is less then 0.01 TPa^{-1}. We found that the z-parameter only decreases by 0.05% over the pressure range of 100 GPa. This implies that the ratio of two inequivalent Be–O bond lengths is constant over the large pressure range (figure 3).

The bulk modulus of 206(3) GPa as obtained from the calculated EOS agrees well with the experimental value of 210(3) GPa [10]. It is also in good agreement with the value of 204 GPa obtained from the calculated elastic stiffness tensor (table 2), which illustrates the high level of internal consistency of the present results.

3.4. Elastic coefficients of BeO

Calculated elastic stiffnesses are shown in table 2 in comparison with the available experimental and theoretical data. The errors quoted for the C_{ij}-values are associated with (i) the deviation

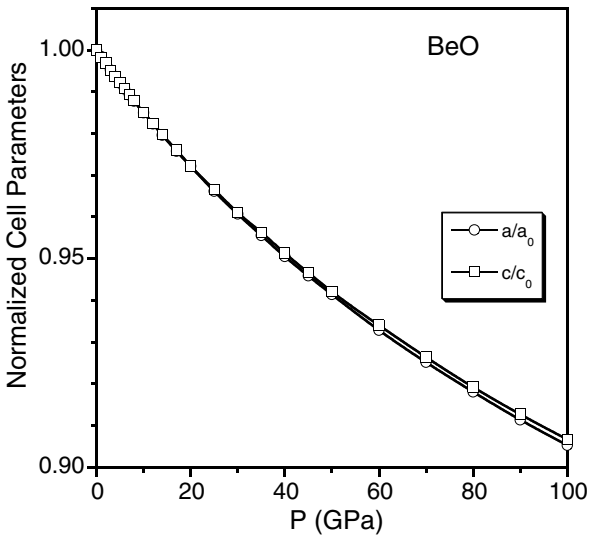

Figure 2. The calculated pressure dependence of the BeO cell parameters normalized to theoretical zero-pressure values (symbols: calculated points; the lines are guides to the eye).

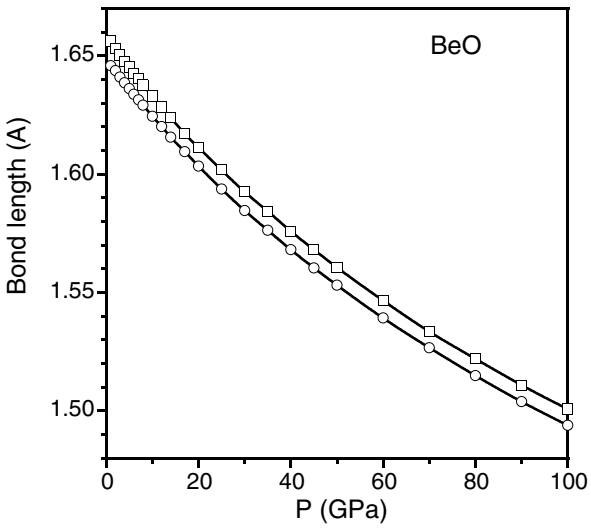

Figure 3. The pressure dependence of two inequivalent Be–O bond lengths (symbols: calculated points; the lines are guides to the eye).

of the stress–strain relationship from linearity, and (ii) the difference between the values of C_{13} obtained from two different strain patterns. The latter error serves as a measure of internal consistency of the calculations, since the two values of C_{13} compared here are obtained from calculations with different crystal symmetry and thus with little scope for fortuitous cancellation of errors. These two values for, e.g., the GGA calculation quoted in table 2 are 71.6 and 72.5 GPa, within the statistical error due to the linear fitting (1 GPa in this case).

It appears from table 2 that the room temperature ultrasonic data [14] and x-ray data [15] are in good agreement with each other. The off-diagonal stiffnesses C_{12} and C_{13} reported in

reference [13] are significantly different from the two other experimental data sets [14, 15], which causes a discrepancy in the C_{66}-value as well. Our calculated values of the diagonal stiffnesses agree with the results of reference [14] to better than 5%, in an obviously better agreement than the Hartree–Fock results [8]. On the other hand, our calculated off-diagonal stiffnesses are 15–20% lower than the experimental values. It is possible that the thermal effects are partially responsible for the deviations, although these effects are expected to be small for oxide ceramics.

A number of incomplete results on elastic coefficients of BeO are available. The compliance component S_{11}, which is the reciprocal of Young's modulus measured in the basal plane, has been reported as 2.33×10^{-3} GPa^{-1} [38]. Similar values were obtained from ultrasonic measurements on single crystals, 2.40×10^{-3} GPa^{-1} [14] and 2.57×10^{-3} GPa^{-1} [13], and on polycrystals, 2.58×10^{-3} GPa^{-1} [39]. The GGA calculations give $S_{11} = 2.46 \times 10^{-3}$ GPa^{-1} in good agreement with the above data. Experimental ultrasonic data for polycrystals with preferred orientations were analysed to extract the values of the compliances S_{33} and $2S_{13} + S_{44}$ from the orientational dependence of Young's modulus [39]. These compliances were reported as 2.17×10^{-3} GPa^{-1} and 5.95×10^{-3} GPa^{-1}, respectively, while our GGA results are 2.29×10^{-3} GPa^{-1} and 6.51×10^{-3} GPa^{-1}. This is a very good agreement, taking into account the fact that the measured compliances include corrections for porosity, Poisson ratio effect, size and shape of samples, not to mention the error of the procedure for extracting single-crystal values from polycrystalline data [39].

The knowledge of the elastic compliances opens an alternative way of evaluating the linear compressibilities [40]:

$$\beta_a = S_{11} + S_{12} + S_{13} \qquad \beta_c = 2S_{13} + S_{33}.$$

These expressions give $\beta_a = 1.62$ TPa^{-1}, $\beta_c = 1.66$ TPa^{-1}. This calculation provides another consistency check for the calculations, since the values obtained from the pressure dependence of the lattice constants and from the elastic compliances should be the same. The corresponding compressibilities calculated from a polynomial fitting in section 3.3 are essentially the same as quoted above (1.63 and 1.62 TPa^{-1}). The two approaches are thus equivalent. It is difficult to establish, on the basis of the available data, which of the two linear compressibilities is higher. The ratio β_a/β_c can be shown to be, in hexagonal crystals,

$$\beta_a/\beta_c = (C_{33} - C_{13})/(C_{11} + C_{12} - 2C_{13}).$$

The relatively low accuracy of the calculated off-diagonal elastic stiffnesses (table 2) prohibits a definitive conclusion on the ordering of the linear compressibilities. Our results thus support the experimental conclusion that the compression is essentially isotropic [10].

We present in table 2 two sets of elastic stiffnesses calculated using the LDA exchange–correlation functional. The first set corresponds to the equilibrium structure as optimized using the LDA, while the second set shows elastic stiffnesses calculated for the experimentally observed structure. The latter structure is essentially equivalent to the ground-state structure calculated using the GGA. The second set of LDA results and the GGA elastic stiffnesses therefore correspond to the same atomic structure, and their comparison is indicative of the effect of the exchange–correlation potential on elastic properties. It follows that high elastic stiffnesses usually attributed to the LDA might be due entirely to the fact that LDA calculations are typically performed for structures with smaller lattice parameters than those used for GGA calculations. In the case of BeO, the effect of this artificial compression is removed, allowing comparison of LDA and GGA results for the same structure and showing that the LDA elastic stiffnesses become noticeably smaller than the GGA ones. We could note in passing that the bulk modulus derived using LDA analysis of the GGA equilibrium structure, 173 GPa, agrees

reasonably well with the estimate of 163 GPa given above, based on the pressure dependence of the bulk modulus.

The discrepancy between various sets of measured and calculated elastic coefficients merits further discussion. The bulk modulus can be deduced from the present study to be 205(2) GPa. This value follows from both the hydrostatic compression data fitted by the third-order equation of state (table 1), and from the data obtained using infinitesimal symmetry-breaking displacements (table 2). This result agrees with the experimental value of 210(3) GPa obtained in hydrostatic compression experiments [10]. A similar value of 214 GPa has been derived from static mechanical tests of polycrystalline samples [41]. The dynamic Young's modulus measured for polycrystals with preferred orientation [42] was later analysed to give $B = 214$ GPa [36], although this result is unreliable in view of the number of approximations made by the authors. Preliminary results of the static measurements on polycrystalline BeO gave 210 GPa [43]. On the other hand, experimental measurements based on ultrasonic techniques [13, 14] give a bulk modulus that is 5–10% higher than hydrostatic results. For example, ultrasonic experiments on polycrystalline samples gave the isothermal bulk modulus of 219 GPa [35, 36] in good agreement with the single-crystal ultrasonic result, 224 GPa [14]. This suggests that the calculated elastic stiffnesses for BeO cannot agree with the experimental ultrasonic values to better than 5–10%, regardless of the quality of the calculation itself.

We expect that the reason for the discrepancies lies in the inherent difference between experimentally measured static and dynamic elastic moduli. It has been shown that dynamic moduli can be up to twice as big as the static ones for rocks and related materials [44, 45]. Noticeably higher dynamic moduli have also been reported for graphitic ceramics [46], shape memory alloys [47], and a number of other materials [48]. It would be interesting to see this issue discussed further by practitioners of the respective experimental techniques.

4. Conclusions

Ultrasoft pseudopotentials within the GGA framework of the density functional theory are shown to provide reliable tools for predicting the structure and mechanical properties of hexagonal BeO. Calculated elastic coefficients confirm that the experimental results of Cline *et al* [14] are more reliable than the earlier data [13]. However, ultrasonic measurements appear to produce an elastic stiffness tensor that is inconsistent with the results of static compression tests and with the theoretical results. Further experimental studies on high-quality single crystals, preferably carried out using a variety of techniques including static testing, might be able to shed more light on this apparent controversy.

Acknowledgments

We are grateful to David Bird and Meri Marlo for their work on implementing the PBE functional in CASTEP, and to Graeme Ackland for the density-of-states linear interpolation package.

References

[1] Vidal-Valat G, Vidal J P, Kurki-Suonio K and Kurki-Suonio R 1987 *Acta Crystallogr.* A **43** 540
[2] Joshi K B, Jain R, Pandya R K, Ahuja B L and Sharma B K 1999 *J. Chem. Phys.* **111** 163
[3] Sabine T M and Hogg S 1969 *Acta Crystallogr.* B **25** 2254
[4] Park C J, Lee S G, Ko Y J and Chang K J 1999 *Phys. Rev.* B **59** 13 501
[5] Van Camp P E and Van Doren V E 1996 *J. Phys.: Condens. Matter* **8** 3385

[6] Chang K J and Cohen M L 1984 *Solid State Commun.* **50** 487
[7] Boettger J C and Wills J M 1996 *Phys. Rev.* B **54** 8965
[8] Lichanot A and Rerat M 1993 *Chem. Phys. Lett.* **211** 249
[9] Jephcoat A P, Hemley R J, Mao H K, Cohen R E and Mehl M J 1988 *Phys. Rev.* B **37** 4727
[10] Hazen R M and Finger L W 1986 *J. Appl. Phys.* **59** 3728
[11] Downs J W, Ross F K and Gibbs G V 1985 *Acta Crystallogr.* B **41** 425
[12] Smith D K, Newkirk H W and Kahn J S 1964 *J. Electrochem. Soc.* **111** 78
[13] Bentle G G 1966 *J. Am. Ceram. Soc.* **49** 125
[14] Cline C F, Dunegan H L and Henderson G W 1967 *J. Appl. Phys.* **38** 1944
[15] Sirota N N, Kuzmina A M and Orlova N S 1990 *Dokl. Akad. Nauk SSSR* **314** 856
[16] Winkler B, Dove M T and Leslie M 1991 *Am. Mineral.* **76** 313
[17] Hohenberg P and Kohn W 1964 *Phys. Rev.* **136** B864
[18] Kohn W and Sham L J 1965 *Phys. Rev.* **140** A1133
[19] Perdew J P and Wang Y 1992 *Phys. Rev.* B **45** 1324
[20] White J A and Bird D M 1994 *Phys. Rev.* B **50** 4954
[21] Perdew J P, Burke K and Ernzerhof M 1996 *Phys. Rev. Lett.* **77** 3865
[22] MSI 1998 *CASTEP User Guide* Molecular Simulations Incorporated, San Diego, CA
[23] Milman V, Winkler B, White J A, Pickard C J, Payne M C, Akhmatskaya E V and Nobes R H 2000 *Int. J. Quantum Chem.* **77** 895
[24] Payne M. C, Teter M P, Allan D C, Arias T A and Joannopoulos J D 1992 *Rev. Mod. Phys.* **64** 1045
[25] Vanderbilt D 1990 *Phys. Rev.* B **41** 7892
[26] Lin J S, Qteish A, Payne M C and Heine V 1993 *Phys. Rev.* B **47** 4174
[27] Zhang L, Ahsbahs H and Kutoglu A 1998 *Phys. Chem. Minerals* **25** 301
[28] Karki B B, Stixrude L, Clark S J, Warren M C, Ackland G J and Crain J 1997 *Am. Mineral.* **82** 635
[29] Karki B B, Stixrude L, Clark S J, Warren M C, Ackland G J and Crain J 1997 *Am. Mineral.* **82** 51
[30] De Vita A, Manassidis I, Lin J S and Gillan M J 1992 *Europhys. Lett.* **19** 605
[31] Monkhorst H J and Pack J D 1976 *Phys. Rev.* B **13** 5188
[32] Akbarzadeh H, Clark S J and Ackland G J 1993 *J. Phys.: Condens. Matter* **5** 8065
[33] Seifert K, Hafner J, Furthmuller J and Kresse G 1995 *J. Phys.: Condens. Matter* **7** 3683
[34] Anderson D L and Anderson O L 1970 *J. Geophys. Res.* **75** 3494
[35] Soga N 1968 *J. Am. Ceram. Soc.* **52** 246
[36] Anderson O L, Schreiber E, Liebermann R C and Soga N 1968 *Rev. Geophys.* **6** 491
[37] Xu Y N and Ching W Y 1993 *Phys. Rev.* B **48** 4335
[38] Austerman S B, Berlincourt D A and Krueger H H 1963 *J. Appl. Phys.* **34** 339
[39] Sjodahl L H and Chandler B A 1963 *J. Am. Ceram. Soc.* **46** 351
[40] Nye J F 1957 *Physical Properties of Crystals: their Representation by Tensors and Matrices* (Oxford: Clarendon)
[41] Bentle G G 1962 *J. Nucl. Mater.* **6** 336
[42] Fryxell R E and Chandler B A 1964 *J. Am. Ceram. Soc.* **47** 283
[43] Ganguly J and Dandekar D P 1985 *10th AIRAPT Int. High Pressure Conf. (Amsterdam)* abstracts, p 17
[44] Jizba D and Nur A 1990 Static and dynamic moduli of tight gas sandstones and their relation to formation properties *Topical Report* prepared for the Gas Research Institute, Tight Gas Sands Project Area, Contract No 5089-211-1842
[45] Walsh J B and Brace W F 1966 *Rock Mech. Eng. Geol.* **4** 283
[46] Oku T and Eto M 1993 *Nucl. Eng. Design* **143** 239
[47] Tonokawa T, Morito S, Nakajima Y, Ooishi A, Otsuka K and Suzuki T 1994 *Japan. J. Appl. Phys.* **1** 2897
[48] Van Heerden W L 1987 *Int. J. Rock Mech. Mining Sci.* **24** 381